Journal of Power Sources 243 (2013) 569–572

Contents lists available at SciVerse ScienceDirect

Journal of Power Sources

journal homepage: www.elsevier.com/locate/jpowsour

Short communication

The influence of self-ordered TiO_2 nanotubes microstructure towards Li^+ intercalation

R.G. Freitas, S.G. Justo, E.C. Pereira*

NANOFAEL, LIEC, Departamento de Química, Universidade Federal de São Carlos, C.P.: 676, CEP: 13565-905, São Carlos, SP, Brazil

HIGHLIGHTS

- TiO_2NTs were prepared using ionic liquid as electrolyte.
- Different tube diameters (21.6, 34.8, 93 and 154.5 nm) were obtained.
- The amount of Li^+ irreversibly trapped was higher in the large TiO_2 nanotubes.
- Smaller the tube diameter the higher the lattice strain during Li-ion intercalation.

GRAPHICAL ABSTRACT

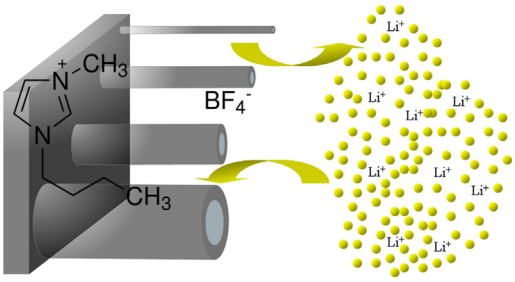

ARTICLE INFO

Article history:
Received 7 May 2013
Received in revised form
4 June 2013
Accepted 4 June 2013
Available online 15 June 2013

Keywords:
TiO_2 nanotube
Li-ion intercalation
Crystallite size
Lattice strain

ABSTRACT

In this work, TiO_2 nanotubes were prepared by anodization at a constant voltage in an electrolyte composed of fluoride species provided by ionic liquid (1 or 5 vol.%), applying 40 or 80 V. Different tube diameters (21.6, 34.8, 93 and 154.5 nm) were obtained, all of them presenting anatase crystalline phase with distinctive crystalline sizes and lattice strains. The Li-ion intercalation/deintercalation was studied and analysed in the light of crystalline structure changes. The amount of Li^+ irreversibly trapped was higher for the samples with larger TiO_2 nanotubes compared to narrower ones. This behaviour was correlated with the lattice strain observed in the samples.

1. Introduction

TiO_2 nanotubes (TiO_2NTs) are a versatile compound and one of the most investigated nanostructures in material science [1]. Synthesis of 1D TiO_2 nanostructures can be achieved using different routes, and among them, electrochemical methods [2,3] associated with solvent-free “green electrolytes” e.g. ionic liquid (IL), can be considered an emergent scientific issue.

ILs are considered powerful solvents and electrically conducting fluids (electrolytes). Salts which are liquid at ambient temperature (e.g., 1-butyl-3-methyl-imidazolium-tetrafluoroborate, BMIM-BF_4) are important for electric battery applications and also, they could act as fluoride species precursors during titanium anodization process. The use of ionic liquid as a source of fluoride species in the electrolyte during the TiO_2NT synthesis process is a quite recent procedure, with few papers reporting their use. Paramasivam et al. [4] observed the formation of well-ordered self-organized TiO_2 nanotubes layers in an electrolyte composed by BMIN-BF_4 ionic liquid as a fluoride precursor. Also, John et al. [5] synthesized double-walled vertically oriented TiO_2 nanotube arrays using sonoelectrochemical anodization in an electrolyte in which fluoride

* Corresponding author. Tel./fax: +55 16 3351 8214.
E-mail addresses: ernesto@ufscar.br, ernestopereira51@gmail.com (E.C. Pereira).

0378-7753/$ – see front matter © 2013 Elsevier B.V. All rights reserved.
http://dx.doi.org/10.1016/j.jpowsour.2013.06.044

species were provided from BMIM-BF_4 ionic liquid. The authors reported the formation of concentric nanotubes under such conditions. In other work, Wender et al. [6] observed that the maximum nanotube growth rate was obtained at 1.0 vol.% BMIM-BF_4 ionic liquid fluoride precursor.

Although ILs are a promising electrolyte for battery application [7], to the best of our knowledge, no paper concerning TiO_2NT prepared using IL electrolytes for Li^+ ion intercalation are described in the literature. As consequence, this paper aims to investigate the synthesis of self-organized TiO_2NTs arrays by anodization in electrolytes composed of BMIM-BF_4 ionic liquid as fluoride precursor. Furthermore, as most of the papers published in the literature concerning Li^+ ion insertion and its relationship with microstructure parameters have a theoretical approach [8–14], this work presents a contribution focused on the correlation between crystallite size, lattice strain and reversibility of the Li^+ ion insertion process on TiO_2NT.

Therefore, we report the growth of TiO_2NT arrays, controlling basically three experimental parameters, i.e. applied voltage, water and BMIM-BF_4 concentration in the electrolyte.

2. Experimental

2.1. Electrode preparation

TiO_2NT arrays were prepared by anodizing 1 cm^2 of titanium foil (99.8% Alfa Aesar) in electrolytes composed of ethylene glycol (Synth), Milli-Q water (10 vol.%), and 1-butyl-3-methyl-imidazolium-tetrafluoroborate (BMIM-BF_4 Sigma–Aldrich) (1 or 5 vol.%). Prior to each anodization, all polished Ti samples were degreased in an ultrasonic bath containing acetone, then rinsed several times in distilled water, and dried in a N_2 stream. Anodization was performed at 25 °C using a standard two-electrode cell with the Ti foil as the anode and platinum foil (4 cm^2) as the cathode, which were kept under a constant applied voltage (40 or 80 V). The voltage was swept from the OCP to different values using 0.1 V s^{-1} as sweep rate. The final voltage was then hold for 120 min. After the anodization process, the samples were rinsed with distilled water and thermally treated at 450 °C for 120 min in order to: eliminate water and organic portions; to improve its mechanical stability; to obtain TiO_2-anatase crystalline structure phase. Just after, a cooling rate of 5 °C min^{-1} was used.

2.2. Electrode characterization

All electrochemical measurements were performed using an Autolab PGSTAT-30 Potentiostat/Galvanostat, under argon controlled atmosphere at room temperature. A platinum wire and TiO_2NTs were respectively used as counter and working electrodes. All potential were referred to Ag quasi electrode. Cyclic voltammetries were carried out using 0.1 M $LiClO_4$ in CH_3CN electrolyte.

The X-ray diffraction (XRD) patterns were obtained using a SIEMENS diffractometer model D-5000 with CuKα radiation and $\lambda = 1.5406$ Å. The morphology of the nanotubes were investigated using field emission scanning electron microscopy (FESEM) (ZEISS microscope, model 105 DSM 940A).

3. Results and discussion

Current–time curves obtained during the formation of the TiO_2 nanotube array films in the BMIM-BF_4 ionic liquid at 40 and 80 V are shown in Fig. 1. Similar current–time profile was observed for all TiO_2NT electrodes: A sharp drop in current is observed during the early stage, due to the formation of an oxide barrier layer [2,3]; followed by an increase in current caused by a fluoride-triggered

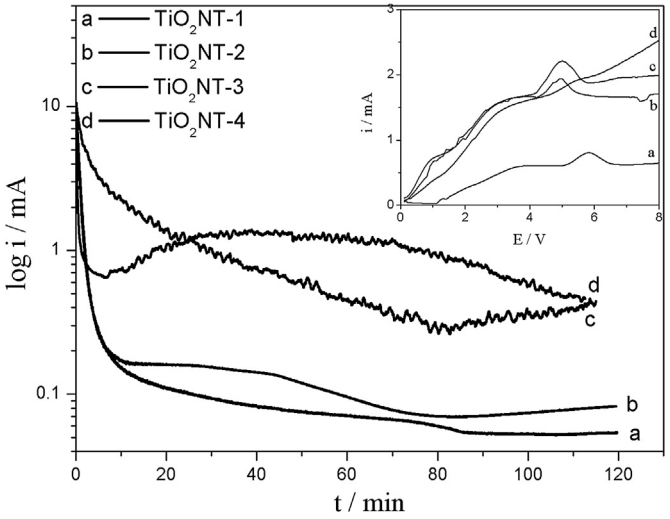

Fig. 1. *I–t* plots during *a*) TiO_2NT-1 (40 V, 1 vol.% IL), *b*) TiO_2NT-2 (40 V, 5 vol.% IL), *c*) TiO_2NT-3 (80 V, 1 vol.% IL) and *d*) TiO_2NT-4 (80 V, 5 vol.% IL). $t = 120$ min. $T = 25$ °C. Inset: initial growth states.

process of oxide layer pitting [2,3], and then finally, current reaches up a steady value. Electrodes TiO_2NT-1 and 2 exhibited lower current values compared to TiO_2NT-3 and 4, which could be related to the lowest voltage values used. Also, it is possible to observe that when using 40 V of applied voltage, the current values increase for higher IL concentration e.g. 1 and 5%, as can be observed for TiO_2NT-1 (40 V and 1 vol.% IL) and TiO_2NT-2 (40 V and 5 vol.% IL). This is in agreement with the reported characteristics of Ti in an F^- containing electrolyte [2]. During the initial voltage sweep towards 40 or 80 V, there is a current increase until about 5 V and then a decrease is observed (Fig. 1 – inset). This is very typical for nanotube formation and can be ascribed to different stages of tube growth [3].

In order to obtain more information about the morphology, FESEM images were acquired for TiO_2NT samples, as shown in Fig. 2.

The average tube diameter obtained at 40 V is near to 21.6 ± 0.7 nm and 34.8 ± 4.2 nm for samples obtained in 1 vol.% and 5 vol.% IL, respectively. For nanotubes obtained at 80 V, the tube diameters are of 93.0 ± 7.4 nm and 154.6 ± 10 nm for samples obtained in 1 vol.% and 5 vol.% IL, respectively. Therefore, the tube diameter can be easily increased if higher IL vol.% and applied voltage are used. Albu et al. [15] also obtained tube diameters of around 40 nm and 100 nm in ethylene glycol electrolyte at 40 and 80 V, respectively. In other work, Wender et al. [6] studied the TiO_2NT formation using ethylene glycol:BMIM-BF_4:water based electrolytes. In the latter, the authors observed an increase in tube diameter when the voltage was raised during the anodization from 20 to 100 V. Paramasivam et al. [4] studied TiO_2NT formation using water miscible and immiscible ionic liquid (i.e. BMIM-X, X = BF_4 and PF_6 respectively). According to the authors, the formation of well-ordered self-organized TiO_2NT layers in BMIM-BF_4 is possible even without additional fluoride addition. In BMIM-PF_6 only the formation of a compact oxide layer was observed. It is in agreement with the data exposed above. Under steady-state conditions, the thickness of the nanotubular oxide layer depends linearly on the anodization time; that is, the charge passed during anodization [2]. Since all samples were prepared using the same anodization time (120 min), the nanotube lengths obtained were 1.6 μm.

The cyclic voltammograms for the Li-ion intercalation/deintercalation process are shown in Fig. 3. Only one pair of cathodic/

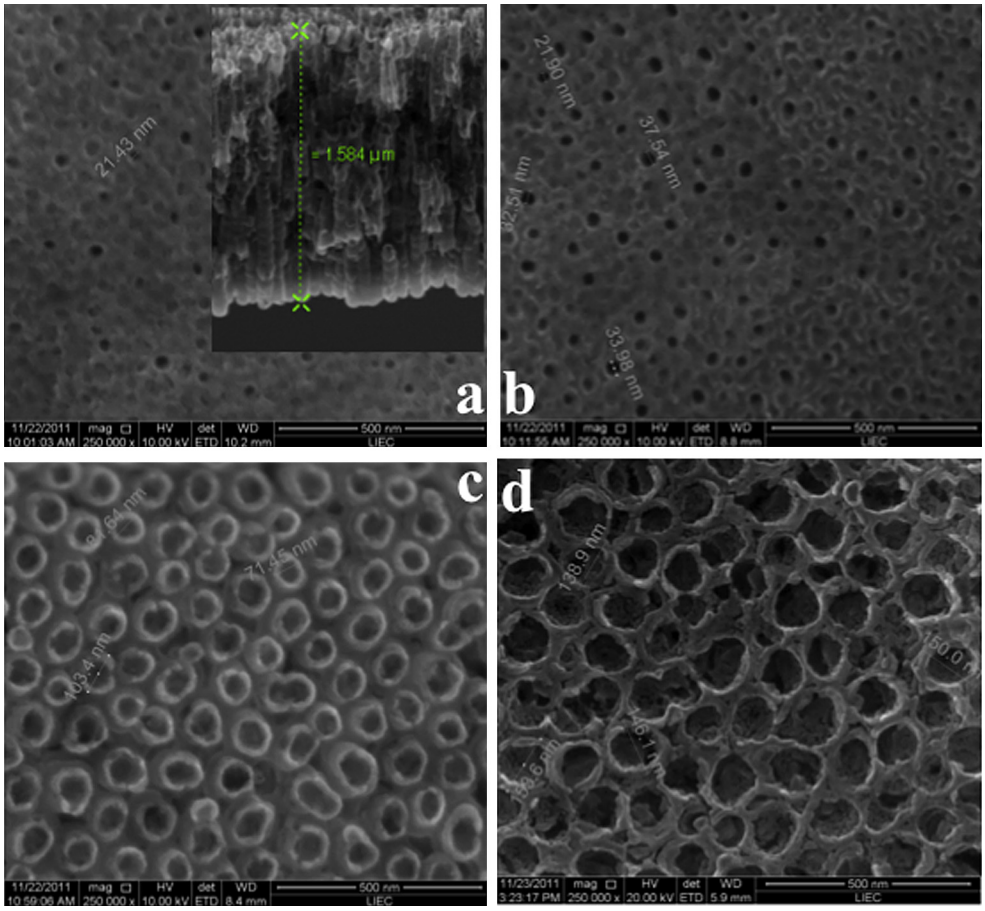

Fig. 2. FESEM images showing TiO_2NTs layers grown by different anodization conditions. Tube diameter: *a*) ~21.6 nm, *b*) 34.8 nm, *c*) 93 nm and *d*) 154.5 nm. Inset: side view of the TiO_2NT layer. $t_{anodization}$ = 120 min.

anodic peaks, located at −1.46 V and −0.84 V (*vs.* Ag), can be observed. The cathodic and anodic peak areas are related to the insertion and extraction of the Li-ion from the TiO_2NTs. The Li-ion insertion/extraction reaction with the TiO_2NT electrodes can be written as:

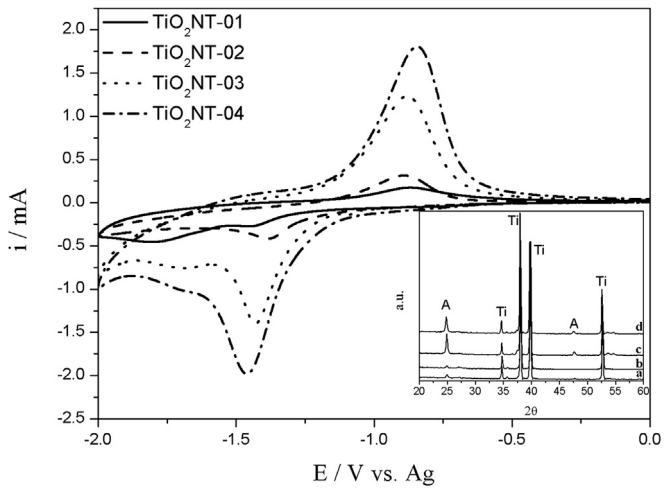

Fig. 3. Cyclic voltammogram of TiO_2NTs in 0.1 M $LiClO_4$ + CH_3CN electrolyte. v = 2 mV s^{-1}. Inset: XRD of TiO_2NTs annealed at 450 °C. A: anatase and Ti: titanium diffraction peak.

$$xLi^+ + xe^- + TiO_2 \leftrightarrow Li_xTiO_2 \quad (1)$$

The insertion coefficient, x, in the anatase crystalline phase is usually closer to 0.5 [16].

As can be observed in the JCPDS-21-1272 data sheet (Fig. 3 – inset), all TiO_2NT presents the TiO_2-anatase crystalline phase at $2\theta = 25.281$ (101). The TiO_2NT self-ordered film was very thin, as shown in Fig. 2 – inset, once titanium peaks were observed (JCPDS-44-1294) at higher intensities than TiO_2-anatase ones.

In Fig. 3, the highest peak current observed was assigned to the TiO_2NT-4 electrode. This sample has the largest tube diameter (154 nm) among those prepared. Therefore, a direct relationship between the tube diameter and the number of available sites for the Li-ion intercalation could reasonably explain the results. However, considering the same surface area, the number of nanotubes for small tube diameters is higher than those expected for large tube diameter samples. Therefore, the above relationship cannot be correct. Nevertheless, considering $Q_{c/a}$ as the cathode and anodic peak quotient obtained from the voltammograms (Fig. 3), values of $Q_{c/a}$ higher than 1 are observed, as the diameter decreases ($Q_{c/a}$ = 1.58, 1.35, 1.2 and 1.0 for TiO_2NT-1, 2, 3 and 4 respectively) meaning that the amount of Li-ion trapped in the TiO_2NTs increases as the tube diameter decreases. Therefore, more Li-ions are trapped in those surfaces whose TiO_2NT tube diameters are smaller. A different explanation can be proposed from the X-ray diffraction data. The crystallite sizes obtained for (101) anatase peak (2θ = 25.281) were of 22.5, 22.8, 29.25 and 33.4 nm [17] for TiO_2NT-1, 2, 3 and 4, respectively (Fig. 3 – inset). In Fig. 4 a

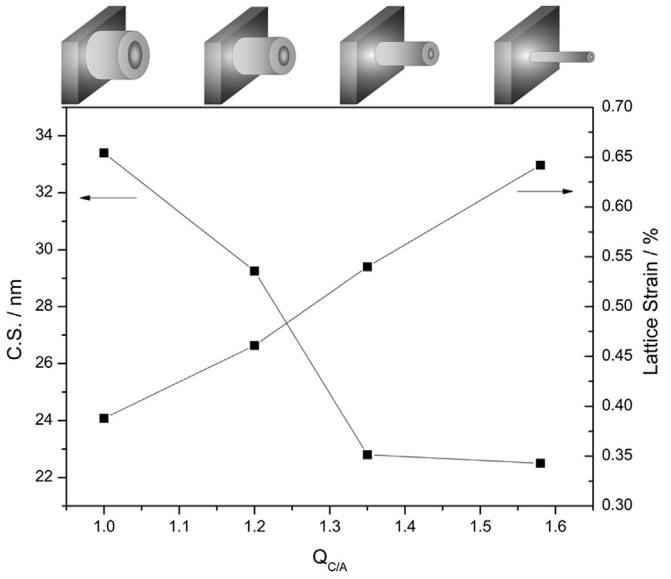

Fig. 4. Crystalline size and lattice strain relation for different Li-ion insertion/extraction in TiO_2NTs.

parametric plot of the CS as a function of $Q_{c/a}$ is presented. It is possible to conclude that the smaller the crystallite size, the higher the Li-ion trapped inside the TiO_2NTs. Besides, Hardwick et al. [18] observed that a phase transition from a tetragonal to an orthorhombic structure takes place at different amounts of Li-ion in the Li_xTiO_2 structure. As a result of this tetragonal–orthorhombic–tetragonal changing structure (during the cyclic voltammetry), the TiO_2NT that exhibits the highest crystallite size i.e. TiO_2NT-4 can modulate the crystalline structure without having several lattice strains and thus, releasing a higher Li-ion content during the deintercalation process.

Although nanoarchitectured materials are interesting materials for Li-ion insertion, the large volume changes upon the lithium ion intercalation/deintercalation causes severe crystallite stresses, which can reduce the cycle ability of the material. Using the Williamson–Hall method [19] to calculate the lattice strain, the values obtained were: 0.642, 0.540, 0.461 and 0.388% for TiO_2NT-1, 2, 3 and 4, respectively, and they are summarized in Fig. 4 as a function of the $Q_{c/a}$ ratio.

In summary, the smaller the TiO_2NT tube diameter, the smaller the crystallite size and therefore the higher the lattice strain during Li-ion intercalation. As an outcome there is a higher number of Li-ions irreversibly trapped in the proper sites. It results in higher $Q_{c/a}$ values for TiO_2NT-1 compared to the TiO_2NT-4 values, as observed in Fig. 3. These propositions are in accordance with Wontcheu et al. [20], who studied the Li-ion intercalation and lattice strain in $Cr_2Ti_3Se_8$ nanomaterials for different Li intercalation degrees, using for that, the Williamson–Hall method [19]. According to the authors [20], a factor of about 6.6 for the increase in the strain among the set of $Cr_2Ti_3Se_8$ materials was observed. Moreover, the authors observed that the values for the lattice strain and changes in the crystallite size depend on the chemical composition of the host materials.

4. Conclusions

The TiO_2NT synthesized upon different conditions (ionic liquid vol.% and applied voltage) lead to distinct tube diameters, as expected. It was observed that the Li-ion ratio trapped in smaller TiO_2NT is higher than in larger ones. This fact was addressed to its smallest crystallite size, which leads to a higher lattice strain due to structural changes of the anatase crystalline phase during the Li-ion insertion.

Acknowledgements

The authors would like to thank the Brazilian Research Funding Institutions CNPq, CAPES, and FAPESP (2010/05555-2 and 2013/07296-2) for financial support.

References

[1] J.M. Macak, H. Tsuchiya, L. Taveira, S. Aldabergerova, P. Schmuki, Angewandte Chemie International Edition 44 (2005) 7463.
[2] J.M. Macak, H. Tsuchiya, A. Ghicov, K. Yasuda, R. Hahn, S. Bauer, P. Schmuki, Current Opinion in Solid State and Materials Science 11 (2007) 3.
[3] J.M. Macak, H. Hildebrand, U.M. Jahns, P. Schmuki, Journal of Electroanalytical Chemistry 621 (2008) 254.
[4] I. Paramasivam, J.M. Macak, T. Selvam, P. Schmuki, Electrochimica Acta 54 (2008) 643.
[5] S.E. John, S.K. Mohapatra, M. Misra, Langmuir 25 (2009) 8240.
[6] H. Wender, A.F. Feil, L.B. Diaz, C.S. Ribeiro, G.J. Machado, P. Migowski, D.E. Weibel, J. Dupont, S.R. Teixeira, Applied Materials Interfaces 3 (2011) 1359.
[7] P.C. Hawett, D.R. MacFarlane, A.F. Hollenkamp, Electrochemical Solid-State Letters 7 (2004) 97.
[8] Z. Cui, F. Gao, J. Qu, Journal of the Mechanics and Physics of Solids 60 (2012) 1280.
[9] X. Xiao, W. Wu, X. Huang, Journal of Power Sources 195 (2010) 7649.
[10] A.F. Bower, P.R. Guduru, V.A. Sethuraman, Journal of the Mechanics and Physics of Solids 59 (2011) 804.
[11] J.L. Zhang, Y.P. Zhao, International Journal of Engineering Science 61 (2012) 156.
[12] R. Fu, M. Xiao, S.Y. Choe, Journal of Power Sources 224 (2013) 211.
[13] T.K. Bhandakkar, H.T. Johnson, Journal of the Mechanics and Physics of Solids 60 (2012) 1103.
[14] A. Awarke, S. Lauer, M. Wittler, S. Pischinger, Computational Materials Science 50 (2011) 871.
[15] S.P. Albu, A. Ghicov, J.M. Macak, P. Schmuki, Physica Status Solidi RRL 1 (2007) R65.
[16] L. Kavan, M. Gratzel, J. Rathousky, A. Zukal, Journal of Electrochemical Society 143 (1996) 394.
[17] B.D. Cullity, Elements of X-ray Diffraction, second ed., Addison-Wesley, New York, 1978.
[18] L.J. Hardwick, M. Holzapfel, P. Novak, L. Dupont, E. Baudrin, Electrochimica Acta 52 (2007) 5357.
[19] A.W. Burton, O. Kenneth, R. Thomas, I.Y. Chan, Microporous and Mesoporous Materials 117 (2009) 75.
[20] J. Wontcheu, W. Bensch, M. Wilkening, P. Heitjans, S. Indris, P. Sideris, C.P. Grey, S. Mankovsky, H. Ebert, Journal of American Chemical Society 130 (2008) 288.